J. Am. Chem. Soc. **1990**, *112*, 1865-1874 1865

Tetraarylporphyrin Sponges. Composition, Structural Systematics, and Applications of a Large Class of Programmable Lattice Clathrates

Marianne P. Byrn, Carol J. Curtis, Saeed I. Khan, Philip A. Sawin, Ryuichi Tsurumi, and Charles E. Strouse*

Contribution from the Department of Chemistry and Biochemistry, J. D. McCullough X-ray Crystallography Laboratory, and the Solid State Science Center, University of California, Los Angeles, California 90024. *Received June 7, 1989*

Abstract: A survey of tetraphenylporphyrins and metallotetraphenylporphyrins reveals that in the solid state many of these compounds adopt a common mode of molecular packing that resembles a simple body-centered-cubic arrangement. The intersecting channels characteristic of this lattice can accommodate a wide range of ligand and solvate "guest" molecules. In this sense, these materials resemble sponges with microscopic pores. Because the axial coordination sites of metalloporphyrin metal atoms are directed into the open channels, these metal atoms can adopt 4-, 5-, or 6-coordinate geometries. Represented in this class are metalloporphyrins with 0, +2, +3, +4, and +5 metal atom oxidation states, as well as free porphyrins with two hydrogen atoms replacing the metal atom. Mixed crystals can be prepared in which the various coordination types and oxidation states coexist. In some such crystals, different chemical species exist in dynamic equilibrium. Simple applications of these materials involve their use to crystallize substances that would otherwise be difficult to obtain in an ordered solid. More sophisticated applications exploit the fact that a host lattice based on materials in this series can be easily tailored to accommodate guests of a predetermined size, shape, handedness, and charge. Structural data are provided for 20 previously unpublished materials.

Because of their structural and electronic relationship to heme complexes, and because of their unusual electronic "flexibility", many synthetic metalloporphyrin complexes have been prepared and subjected to intensive structural and spectroscopic characterization. The 1988 version of the Cambridge Structural Database[1] includes more than 150 compounds containing the tetraphenylporphinato (TPP) ligand. Since the TPP ligand is large and relatively rigid, interactions among adjacent porphyrin ligands tend to govern the crystal packing. Anticipating the degree to which these interactions control the composition and structure of crystalline TPP complexes, Scheidt and Lee[2] recently identified several closely isostructural series of TPP complexes. Reported herein, an examination of the structures of both new and previously reported TPP complexes reveals a larger group of complexes with a variety of space groups but with a common mode of packing. Table I contains lattice parameters for 65 "isostructural" TPP complexes.[42]

Particularly striking is the enormous chemical diversity rep-

---

(1) Allen, F. H.; Kennard, O.; Taylor, R. *Acc. Chem. Res.* **1983**, *16*, 146-153.

(2) Scheidt, W. R.; Lee, Y. J. *Struct. Bond.* (*Berlin*) **1987**, *64*, 1-70.

(3) Abbreviations used herein: amyl, isoamyl; BzImH, benzimidazole; Et, ethyl; F_4Ph, 2,3,5,6-tetrafluorophenyl; MBS, methyl benzyl sulfide; Me, methyl; 2-MeIm^+, 2-methylimidazolium; *o*-NH_2TPP, tetraphenylporphinato with a single *o*-amino substituent; THF, tetrahydrofuran; Tol, tolyl; TPP, tetraphenylporphinato.

(4) Drew, M. G. B.; Mitchell, P. C. H.; Scott, C. E. *Inorg. Chim. Acta* **1984**, *82*, 63-68.

(5) Budge, J. R.; Gatehouse, B. M. K.; Nesbit, M. C.; West, B. O. *J. Chem. Soc., Chem. Commun.* **1981**, 370-371.

(6) Schneider, M. L. *J. Chem. Soc., Dalton Trans.* **1972**, 1093-1096.

(7) Anzai, K.; Hatano, K.; Lee, Y. J.; Scheidt, W. R. *Inorg. Chem.* **1981**, *20*, 2337-2339.

(8) Timkovich, R.; Tulinsky, A. *J. Am. Chem. Soc.* **1969**, *91*, 4430-4432.

(9) Glick, M. D.; Cohen, G. H.; Hoard, J. L. *J. Am. Chem. Soc.* **1967**, *89*, 1996-1998.

(10) Scheidt, W. R.; Hoard, J. L. *J. Am. Chem. Soc.* **1973**, *95*, 8281-8288.

(11) Scheidt, W. R.; Frisse, M. E. *J. Am. Chem. Soc.* **1975**, *97*, 17-21.

(12) Sakurai, T.; Yamamoto, K. *Sci. Pap. Inst. Phys. Chem. Res.* (*Jpn.*) **1976**, *70*, 31-37.

(13) Ledon, H.; Mentzen, B. *Inorg. Chim. Acta* **1978**, *31*, L393-L394.

(14) Hoard, J. L.; Cohen, G. H.; Glick, M. D. *J. Am. Chem. Soc.* **1967**, *89*, 1992-1996.

(15) Sakurai, T.; Yamamoto, K.; Naito, H.; Nakamoto, N. *Bull. Chem. Soc. Jpn.* **1976**, *49*, 3042-3046.

(16) Collins, D. M.; Scheidt, W. R.; Hoard, J. L. *J. Am. Chem. Soc.* **1972**, *94*, 6689-6696.

(17) Lecomte, C.; Protas, J.; Marchon, J. C.; Nakajima, M. *Acta Crystallogr., Sect. B* **1978**, *B34*, 2856-2858.

(18) Scheidt, W. R.; Mondal, J. U.; Eigenbrot, C. W.; Adler, A.; Radonovich, L. J.; Hoard, J. L. *Inorg. Chem.* **1986**, *25*, 795-799.

(19) Silvers, S. J.; Tulinsky, A. *J. Am. Chem. Soc.* **1967**, *89*, 3331-3337.

(20) Bonnet, J. J.; Eaton, S. S.; Eaton, G. R.; Holm, R. H.; Ibers, J. A. *J. Am. Chem. Soc.* **1973**, *95*, 2141-2149.

(21) Schauer, C. K.; Anderson, O. P.; Eaton, S. S.; Eaton, G. R. *Inorg. Chem.* **1985**, *24*, 4082-4086.

(22) Reed, C. A.; Mashiko, T.; Scheidt, W. R.; Spartalian, K.; Lang, G. *J. Am. Chem. Soc.* **1980**, *102*, 2302-2306.

(23) Rodesiler, P. F.; Griffith, E. H.; Ellis, P. D.; Amma, E. L. *J. Chem. Soc., Chem. Commun.* **1980**, 492-493.

(24) Radonovich, L. J.; Bloom, A.; Hoard, J. L. *J. Am. Chem. Soc.* **1972**, *94*, 2073-2078.

(25) Magurany, C. J. M.S. Thesis, UCLA, 1982; p 34.

(26) Scheidt, W. R. *J. Am. Chem. Soc.* **1974**, *96*, 84-89.

(27) Collman, J. P.; Barnes, C. E.; Brothers, P. J.; Collins, T. J.; Ozawa, T.; Gallucci, J. C.; Ibers, J. A. *J. Am. Chem. Soc.* **1984**, *106*, 5151-5163.

(28) McKee, V.; Ong, C. C.; Rodley, G. A. *Inorg. Chem.* **1984**, *23*, 4242-4248.

(29) Cocolios, P.; Lagrange, G.; Guilard, R.; Oumous, H.; Lecomte, C. *J. Chem. Soc., Dalton Trans.* **1984**, 567-574.

(30) Miller, K. M. Ph.D. Thesis, UCLA, 1983.

(31) Katz, B. A. Ph.D. Thesis, UCLA, 1979.

(32) Byrn, M. P.; Strouse, C. E., to be published.

(33) Scheidt, W. R.; Kastner, M. E.; Hatano, K. *Inorg. Chem.* **1978**, *17*, 706-714.

(34) Kirner, J. F.; Reed, C. A.; Scheidt, W. R. *J. Am. Chem. Soc.* **1977**, *99*, 1093-1101.

(35) Burstyn, J. N. Ph.D. Thesis, UCLA, 1986; p 150.

(36) Levan, K. R. Ph.D. Thesis, UCLA, 1984.

(37) Scheidt, W. R.; Lee, Y. J.; Tamai, S.; Hatano, K. *J. Am. Chem. Soc.* **1983**, *105*, 778-782.

(38) Harrison, P. G.; Molloy, K.; Thornton, E. W. *Inorg. Chim. Acta* **1979**, *33*, 137-144.

(39) Scheidt, W. R.; Cunningham, J. A.; Hoard, J. L. *J. Am. Chem. Soc.* **1973**, *95*, 8289-8294.

(40) Riche, C.; Chiaroni, A.; Gouedard, M.; Gaudemer, A. *J. Chem. Res.* **1978**, *32*, 534-545.

(41) Mashiko, T.; Reed, C. A.; Haller, K. J.; Scheidt, W. R. *Inorg. Chem.* **1984**, *23*, 3192-3196.

(42) The search for structural similarity that produced this table was exhausting, but not exhaustive. There are undoubtedly other published TPP structures that could be included in this group. There are groups of monoclinic materials and groups of triclinic $Z = 2$ materials whose structures are closely related to those of the materials tabulated in Table I. An on-going effort in this laboratory is designed to catalog additional members of this series, and to explore structural relationships in other similar series.

0002-7863/90/1512-1865$02.50/0

Table I

(a) Lattice Parameters for Body-Centered Tetragonal TPP Complexes

M–ligand	*a*	*c*	*V*	d_{002} (ref)	M–ligand	*a*	*c*	*V*	d_{002} (ref)
$\mathrm{V^{+4}O}$	13.345	9.745	1736	4.872 (4)	$\mathrm{Co^{+3}Cl}$	13.489	9.779	1779	4.890 (12)
$\mathrm{Cr^{+4}O}$	13.351	9.749	1738	4.874 (5)	$\mathrm{Co^{+3}Br}$	13.460	9.840	1783	4.920 (12)
$\mathrm{Ag^{+2}{}_{0.54}2H^{+}{}_{0.46}}$	13.384	9.717	1741	4.858 (6)	$\mathrm{Mo^{+5}OCl}$	13.469	9.852	1787	4.926 (13)
$\mathrm{Fe^{+3}F}$	13.381	9.767	1749	4.884 (7)	$\mathrm{Fe^{+3}Cl}^{h}$	13.534	9.820	1799	4.910 (14)
$\mathrm{Mg^{+2}H_2O}$	13.460	9.680	1754	4.840 (8)	$\mathrm{Co^{+3}Cl}^{h}$	13.693	9.701	1819	4.850 (15)
$\mathrm{Zn^{+2}H_2O}$	13.440	9.715	1755	4.858 (9)	$\mathrm{Sn^{+4}Cl_2}$	13.673	9.961	1862	4.980 (16)
$\mathrm{Co^{+2}NO}$	13.434	9.754	1760	4.877 (10)	$\mathrm{Ti^{+4}Br_2}$	13.757	9.880	1870	4.940 (17)
$\mathrm{Fe^{+2}NO}$	13.468	9.755	1769	4.878 (11)					

(b) Body-Centered Lattice Parameters for Triclinic TPP Complexes[g]

M–ligands–solvate[a]	*a*	*b*	*c*	α	β	γ	V^{b}	d_{002} (ref)[c]
$\mathrm{Zn^{+2}}$	14.903	26.548	11.109	74.11	23.35	68.44	1596	2.169 (18)
$\mathrm{2H^{+}}$	14.922	26.614	11.142	74.11	23.33	68.11	1597	2.168 (19)
$\mathrm{Ag^{+2}}$	14.907	26.580	11.223	74.05	23.07	68.75	1603	2.170 (18)
$\mathrm{Ru^{+2}(CO)EtOH}$	14.651	13.313	10.079	100.20	79.03	79.05	1848	4.825 (20)
$\mathrm{2H^{+}}$*p*-xylene	13.667	17.692	14.470	60.85	43.34	80.94	1981	4.148 (tw)
$\mathrm{Zn^{+2}(THF)_2}$	13.248	17.609	12.320	65.57	51.38	76.07	(2044)	4.513 (21)
$\mathrm{Zn^{+2}}$(trioxane)$_2$	13.397	17.341	13.258	65.60	47.94	81.03	2049	4.465 (tw)
$\mathrm{Fe^{+2}(THF)_2}$	13.348	17.665	12.388	66.09	52.19	76.29	2110	4.605 (22)
$\mathrm{Zn^{+2}}$phenanthrene	13.319	19.406	13.087	58.47	47.87	74.58	2119	4.252 (tw)
$\mathrm{Cd^{+2}}$(1,4-dioxane)$_2$	13.488	17.790	12.412	64.67	52.88	74.76	2146	4.636 (23)
$\mathrm{Fe^{+2}}$(piperidine)$_2$	13.334	18.230	12.747	65.97	50.37	76.04	2179	4.618 (24)
$\mathrm{Fe^{+3}}$(amylS$^-$)amylSH	13.595	17.203	10.984	76.40	63.45	74.46	(2194)	4.868 (25)
$\mathrm{Co^{+2}}$(piperidine)$_2$	13.335	18.144	12.531	65.73	52.70	75.64	2199	4.690 (26)
$\mathrm{Ru^{+3}(EtO^-)(EtOH)_3}$	13.389	24.000	9.894	72.13	46.64	76.83	(2199)	3.514 (27)
$\mathrm{Mg^{+2}}$(piperidine)$_2$	13.459	18.163	12.580	65.75	52.10	75.56	2212	4.673 (28)
$\mathrm{Fe^{+3}(PhSO_2{}^-)}^{d}$	13.330	21.084	11.733	58.93	51.64	71.16	2215	4.163 (29)
$\mathrm{Fe^{+3}(F_4PhS^-)F_4PhSH}$	13.511	21.723	11.594	63.27	46.88	73.58	(2217)	3.937 (30)
$\mathrm{Mg^{+2}}$(4-picoline)$_2$	13.511	17.773	12.388	66.57	54.41	74.34	2217	4.794 (28)
$\mathrm{Fe^{+3}(PhS^-)PhSH}$	13.473	21.189	11.707	60.71	49.88	71.52	2229	4.116 (31)
$\mathrm{Fe^{+3}}$(*m*-MePhS$^-$)*m*-MePhSH	13.302	21.382	12.297	58.18	48.75	71.43	(2232)	4.140 (31)
$\mathrm{Fe^{+3}(PhS^-)}$chlorobenzene	13.492	21.161	11.736	60.67	49.85	71.47	2233	4.124 (32)
$\mathrm{Zn^{+2}}$(toluene)$_2$	13.488	21.516	11.349	63.99	49.10	73.88	2237	4.012 (33)
$\mathrm{Zn^{+2}}$(phenylacetylene)$_2$	13.518	20.655	12.958	56.81	47.94	71.23	2242	4.241 (tw)
$\mathrm{Mn^{+2}}$(toluene)$_2$	13.541	21.591	11.321	64.11	48.90	73.80	2244	3.996 (34)
$\mathrm{Fe^{+3}(PhS^-)}$toluene	13.493	21.336	11.679	61.12	49.74	71.92	2247	4.105 (32)
$\mathrm{Fe^{+3}(PhCO_2{}^-)}$toluene	13.426	20.861	12.036	58.11	51.92	70.78	2253	4.259 (35)
$\mathrm{Fe^{+3}}$(benzylS$^-$)benzylSH	13.437	17.337	11.483	75.05	63.29	73.35	2263	5.070 (36)
$\mathrm{Fe^{+3}}$(*o*-$\mathrm{NH_2TPP)(PhS^-)PhSH}$	13.478	21.178	11.684	61.57	50.60	71.36	2265	4.188 (30)
$\mathrm{Zn^{+2}}$(styrene)$_2{}^{e}$	13.471	21.688	11.435	63.12	50.04	73.96	2284	4.067 (tw)
$\mathrm{Zn^{+2}}$(*o*-xylene)$_2$	13.677	21.975	10.975	66.94	49.16	72.97	2292	3.989 (tw)
$\mathrm{Zn^{+2}}$(1,5-cyclooctadiene)$_2$	13.289	19.352	11.632	68.32	56.07	73.10	(2293)	4.659 (tw)
$\mathrm{2H^{+}}$(*m*-xylene)$_2$	13.632	19.389	12.020	54.87	63.11	70.97	2308	4.619 (tw)
$\mathrm{Zn^{+2}}$(*m*-xylene)$_2$	13.465	21.709	11.174	64.80	51.98	72.99	2326	4.161 (tw)
$\mathrm{Fe^{+3}(F^-)_2(2\text{-}MeIm^+)(CHCl_3)_2}$	16.786	20.106	13.609	60.05	36.96	58.78	2329	4.035 (37)
$\mathrm{Fe^{+3}}$(*p*-MePhS$^-$)(*p*-MePhSH)	13.421	21.840	11.919	58.72	51.37	71.43	2332	4.197 (31)
$\mathrm{Zn^{+2}}$(ethylbenzene)$_2$	13.518	21.696	11.488	63.52	51.06	74.19	2345	4.156 (tw)
$\mathrm{Zn^{+2}}$(3-methylanisole)$_2{}^{f}$	13.422	21.841	11.479	61.92	52.65	72.15	2359	4.227 (tw)
$\mathrm{Zn^{+2}}$(methylbenzoate)$_2$	13.482	21.210	12.535	55.72	52.83	69.70	2360	4.400 (tw)
$\mathrm{Zn^{+2}}$(1,5-cyclooctadiene)$_2$	13.472	19.437	11.910	66.83	55.74	73.63	2362	4.701 (tw)
$\mathrm{Zn^{+2}}$(1,2,4-trimethylbenzene)$_2$	15.190	23.414	12.539	47.58	46.41	62.32	2385	3.786 (tw)
$\mathrm{Zn^{+2}}$(2,5-(Me)$_2$-2,4-hexadiene)$_2$	14.848	24.156	11.995	51.19	46.19	64.03	2419	3.751 (tw)
$\mathrm{Zn^{+2}}$(*m*-ethylvinylbenzene)$_2$	13.604	22.249	11.337	60.59	54.45	69.62	2422	4.269 (tw)
$\mathrm{Zn^{+2}}$(ethylbenzoate)$_2$	13.613	24.915	19.265	42.44	38.59	66.97	2469	3.955 (tw)
$\mathrm{Fe^{+3}(H_2O)_2ClO_4{}^-}$(MeSbenzyl)	12.865	23.586	10.165	107.25	71.55	74.24	(2557)	4.377 (36)
$\mathrm{Sn^{+4}(OH^-)_2(CHCl_3)_2(CCl_4)_2}$	15.921	27.463	12.229	38.09	57.21	74.54	2638	3.130 (38)
$\mathrm{Zn^{+2}}$(*p*-ethoxyethyl benzoate)$_2$	13.679	23.808	16.693	45.19	52.67	80.66	2706	4.211 (tw)
$\mathrm{Fe^{+3}(BzImH)_2ClO_4{}^-}$toluene	17.826	17.145	11.967	78.96	49.47	81.13	(2726)	4.514 (36)
$\mathrm{Co^{+3}}$(piperidine)$_4\mathrm{NO_3{}^-}$	13.476	26.587	15.479	52.22	41.41	67.88	2862	4.312 (39)
$\mathrm{Co^{+3}(PhEtNH)_2Br^-(CHCl_3)_2}$	17.150	22.991	14.300	61.21	38.04	57.44	2910	4.378 (40)
$\mathrm{Fe^{0}(Na^{+}(THF)_3)_2}$	18.620	22.537	15.768	49.99	36.99	62.55	3030	4.068 (41)

[a] Abbreviations are given in ref 3. [b] Volume in parentheses indicates low-temperature structure determination. [c] tw indicates this work. [d] This material probably contains a toluene of solvation. [e] The vinyl group of the styrene exhibits a 2-fold disorder. [f] The 3-methylanisole group is disordered by an approximate interchange of the methyl and methoxy groups. [g] Transformation matrices from the unit cells in which the structures were originally determined can be found in the supplementary material. [h] See footnote 43.

resented in this group of materials. The common lattice structure accommodates a wide range of ligand and solvate molecules, metal atom coordination numbers, and metal atom oxidation states. Cursory examination of packing diagrams reveals the potential of these TPP materials as clathrate "hosts". The occurrence of the ligand and/or solvate "guest" molecules in extended channels suggests a number of applications exploiting the fact that interactions among the guest molecules are usually restricted to a single dimension. Perhaps most intriguing, however, is a feature of this structure that allows the host lattice to be easily "programmed" to preferentially incorporate guest molecules of a *predetermined* size, shape, handedness, and charge. The goals of the present report are to explore the range of composition of this class of materials, to examine the structural systematics, to report the synthesis and structure determination of 20 new materials, and to illustrate, by way of several examples, potential applications

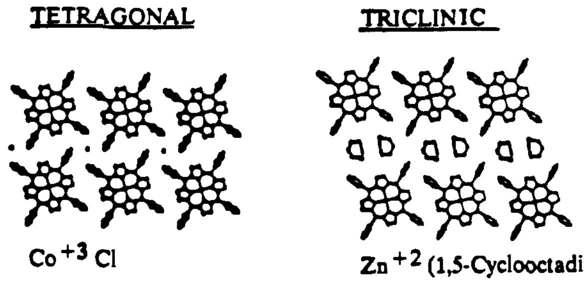

Figure 1. Typical examples of the body-centered tetragonal materials tabulated in Table Ia and the triclinic materials tabulated in Table Ib. In this and similar figures, a section of the structure parallel to the crystallographic *a* and *b* axes is shown. The *a* axis extends from left to right, and the *b* axis extends from top to bottom. All unit cells are body-centered ($Z = 2$); the axial ligands in these drawings are coordinated to metalloporphyrins related by body-centering operations to those shown.

of this large class of clathrates.

Experimental Section

Preparations. Preparation of porphyrin or metalloporphyrin clathrates usually consists simply of recrystallization of the host material from the desired guest. Typically, a saturated solution is prepared above room temperature and allowed to cool slowly to room temperature. With high-melting guests, the crystals can be grown either at elevated temperature from the melt or near room temperature from a nonincorporating solvent. Saturated hydrocarbons and halocarbons are not usually incorporated and are thus suitable solvents for such crystallizations.

One can sometimes induce adoption of the triclinic 1:2 (vide infra) structure by seeding the saturated solution with crystallites of a chemically similar material having the desired structure.

Porphyrins used in this investigation were obtained from Midcentury; guests and solvents were obtained from Aldrich. Unleaded gasoline was obtained from Unocal 76.

Instrumental Analysis. All X-ray measurements were made with locally automated Huber, Syntex, and Picker diffractometers. One Huber diffractometer is equipped with a closed-cycle Air Products refrigerator, and the Picker diffractometer is equipped with a gas stream low-temperature device. All crystals were coated with epoxy to prevent loss of solvate. Crystallographic data for 20 new clathrates are provided in the supplementary material.

Analyses of solvent and solvate mixtures made use of an HP 5890A gas chromatograph. Thermogravimetric analyses made use of a Du Pont 951 analyzer.

Results and Discussion

Structural Systematics. Tetragonal Materials. Table Ia lists 15 tetragonal TPP complexes in order of increasing unit cell volume. These materials are either 5-coordinate complexes with axial ligands containing one or two non-hydrogen atoms or 6-coordinate complexes with two monoatomic ligands. With the exception of the thirteenth compound in the list, they have all been refined in the centrosymmetric space group *I*4/*m*, which imposes a disorder on the 5-coordinate complexes. With two exceptions,[43] there is a good correlation between the unit cell volumes and the number and size of the axial ligand atoms. The first structure in Figure 1 is representative of this group of materials.

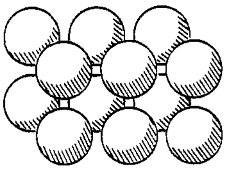

Figure 2. A simple body-centered-cubic structure.

Triclinic Materials. If the triclinic materials tabulated in Table Ib are described within the framework of reduced triclinic cells, any structural similarity is difficult to detect. If, however, "similar" body-centered unit cells are chosen, the structural relationships can be easily described in terms of distortions of the body-centered tetragonal cell exhibited by the materials tabulated in Table Ia. It is useful to take this generalization one step further. The gross packing of TPP molecules in all these materials resembles a simple body-centered-cubic (BCC) arrangement. A simple BCC structure is not close-packed; it contains a network of intersecting channels parallel to the three coordinate axes (see Figure 2). In the porphyrin-based materials examined herein, ligand and solvate molecules can be thought of as occupying the channels of such a spongelike framework. Recognition of the common features of these structures leads to some simple and potentially powerful predictions concerning interactions between specific hosts and guests.

When *a* and *b* axes of the triclinic cell are chosen to be nearly parallel to the porphyrin plane, all the materials in Table Ib exhibit a packing arrangement in the *ab* plane typified by the second structure in Figure 1. In one direction (assigned as the *a* direction), chains of translationally equivalent porphyrin molecules are observed with relative orientations similar to those in the tetragonal materials and with typical repeat distances of 13–14 Å.

A common feature of these chains is the interaction between perpendicularly oriented phenyl groups on neighboring molecules. The distance between the centroids of these interacting phenyl groups is ca. 5.2–5.3 Å, similar to the most common distance between aromatic residues in proteins[44] of ~5.5 Å, and the minimum distance of 5.0 Å observed between the centroids of nearly orthogonal molecules in solid benzene.[45] A stabilization of approximately 1 kcal/mol has been attributed to these interactions.[44]

Parallel chains of porphyrin molecules in the *ab* plane are separated by channels occupied by ligand and/or solvate molecules. The occupation of these channels results in *b* lattice parameters ranging from 13 to 27 Å. The angle between *a* and *b* in these materials is typically 65–75°, with a few values falling outside this range.

Occupation of the channel parallel to *a* also has a systematic effect on the geometry in the third dimension; the α and β lattice angles for the shortest choice of *c* consistent with a body-centered cell are typically in the range 50–70°. The combined distortions correspond to an elongation of the tetragonal cell along the body diagonal.

Unsubstituted Rings. Figure 3 illustrates the molecular packing of eight materials in which the "guest" species are unsubstituted cyclic molecules. These include 1,5-cyclooctadiene, THF, dioxane, trioxane, and piperidine. Notable by its absence from this list is benzene. Benzene can indeed be incorporated into ZnTPP, but this clathrate adopts a monoclinic structure.[46]

Monosubstituted Rings. Figures 4 and 5 illustrate the molecular packing of materials in which the guest molecules are monosubstituted six-membered rings. The orientations of these guests fall

---

[43] The first anomalous result in Table Ia involves compound FeTPPCl, which gives a unit cell volume larger than one would expect by comparison to similar compounds. This is almost certainly a mixed crystal. It was originally reported as FeTPP(OH)(H_2O) and later reinterpreted as containing at least a significant fraction of FeTPPCl. However, refinement based on a FeTPPCl model gave a displacement of the iron atom from the porphyrin plane smaller than that observed in the analogous F and Br complexes. The second anomaly involves the second entry labeled CoTPPCl. With a unit cell volume ~50 $Å^3$ larger than that obtained in the other determination, it seems likely that this complex has a water (or perhaps methanol) molecule in the site opposite the chloride ion. This complex was refined in the space group *I*4, and the authors attributed the difference in lattice parameters to the difference between ordered and disordered structures. It seems likely, however, that the difference in lattice parameters and the putative difference in space group are associated with a difference in composition. Two other observations are pertinent. First, the elemental analysis given for this material is consistent with ca. 0.5 mol of water per molecule. Second, the *a* lattice parameter is larger than those of all the tetragonal 5-coordinate complexes in Table I and very similar to that of the two 6-coordinate symmetrically ligated complexes. A third determination of the structure of CoTPPCl, with a unit cell volume of 1766 $Å^3$, was reported in a review article by: Fleischer, E. B. *Acc. Chem. Res.* **1970**, *3*, 105.

[44] Burley, S. K.; Petsko, B. A. *Science* **1985**, *229*, 23–28.

[45] (a) Bacon, B. E.; Curry, N. A.; Wilson, S. A. *Proc. R. Soc. London, A* **1964**, *279*, 98–110. (b) Williams, D. E. *Acta Crystallogr.* **1980**, *A36*, 715–723.

[46] Crystallographic data for this clathrate are found in the supplementary material.

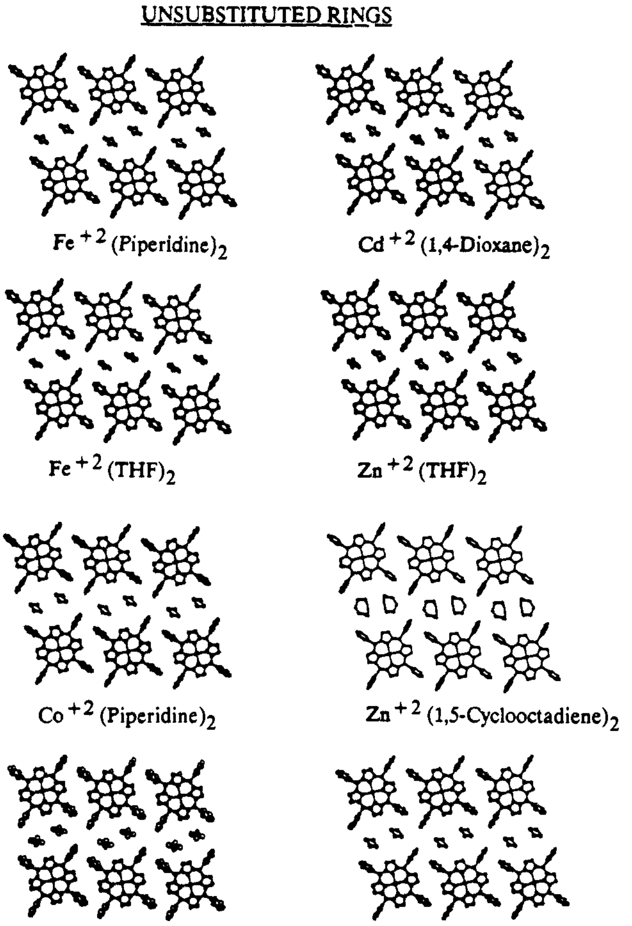

UNSUBSTITUTED RINGS

$Fe^{+2}(Piperidine)_2$ $Cd^{+2}(1,4\text{-}Dioxane)_2$

$Fe^{+2}(THF)_2$ $Zn^{+2}(THF)_2$

$Co^{+2}(Piperidine)_2$ $Zn^{+2}(1,5\text{-}Cyclooctadiene)_2$

$Zn^{+2}(Trioxane)_2$ $Mg^{+2}(Piperidine)_2$

Figure 3. Porphyrin sponges containing cyclic unsubstituted guests.

into two categories, designated A and B. In category A, the substituents adopt orientations that can be described as 8 o'clock and 2 o'clock with respect to the *a* direction. The corresponding guests in the B category adopt 4 o'clock and 10 o'clock orientations. In all cases, the long direction of the molecule is directed approximately normal to the channel direction, resulting in a repeat distance in the channel direction commensurate with the 13.5-Å spacing of the porphyrin hosts.

Disubstituted Rings. Figure 6 illustrates the packing of a number of disubstituted benzene guest species. The meta-substituted guests adopt geometries in which the substituent atoms of one guest are at approximately 4 o'clock and 8 o'clock with respect to the *a* direction, while those of the second guest are at approximately 10 o'clock and 2 o'clock. This corresponds to one combination of the A and B geometries observed for the monosubstituted rings.[47] Similarly, the ortho-substituted guests adopt orientations in which the substituents of one guest are at the 2 o'clock and 4 o'clock orientations with respect to *a*, while those of the second guest are at 8 o'clock and 10 o'clock. The para-substituted rings adopt the "compromise" 3 o'clock–9 o'clock orientation.

Double Chains. The materials in Figure 7 adopt a structure in which the channel in the *a* direction contains a double row of guests. For the ethyl benzoate and ethyl ethoxybenzoate guests, the driving force for this arrangement appears to be an approximate match between the long dimension of the guest and the porphyrin repeat distance along *a*. This, however, does not account for those "double chains" made up of a larger number of smaller guests.

1:1 Clathrates. While most clathrates in this series have a 1:2 host:guest stoichiometry, Figure 8 shows two materials with the

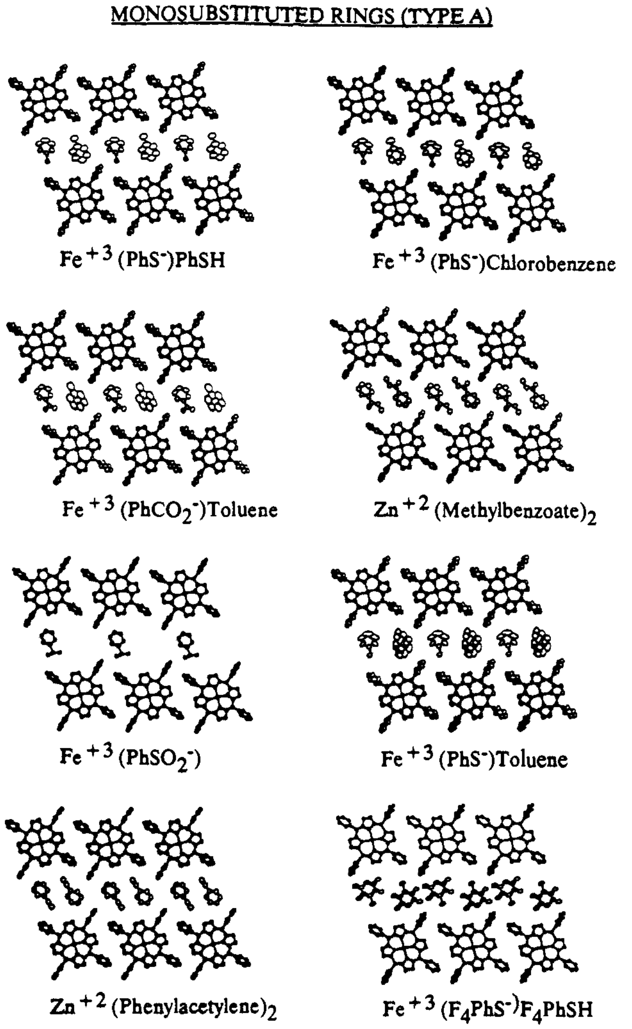

MONOSUBSTITUTED RINGS (TYPE A)

$Fe^{+3}(PhS^-)PhSH$ $Fe^{+3}(PhS^-)Chlorobenzene$

$Fe^{+3}(PhCO_2^-)Toluene$ $Zn^{+2}(Methylbenzoate)_2$

$Fe^{+3}(PhSO_2^-)$ $Fe^{+3}(PhS^-)Toluene$

$Zn^{+2}(Phenylacetylene)_2$ $Fe^{+3}(F_4PhS^-)F_4PhSH$

Figure 4. Porphyrins sponges containing monosubstituted six-membered rings (type A).

same gross structure but with a 1:1 stoichiometry. For the H_2TPP *p*-xylene clathrate, it might seem that the 1:1 stoichiometry is favored by the inversion symmetry of the guest, but this is clearly not the case for the ZnTPP phenanthrene clathrate. Further, preparation of the ZnTPP *p*-xylene clathrate results in the spontaneous crystallization of a material[46] with 2:1 stoichiometry, and if this solution is seeded with crystallites of the 1:2 ZnTPP *o*-xylene clathrate, crystals of 1:2 stoichiometry are produced.

Large d_{002} Materials. The isoamyl and benzyl thiol/thiolate complexes of $Fe^{III}TPP$ appear to exhibit a strong pairwise interaction between guest species (see Figure 9). This interaction is associated with an expansion of the interplanar spacing (d_{002}) of the host. The materials in the following section exhibit the opposite distortion of the host.

Unsolvated Species. The unit cells chosen for the unsolvated triclinic forms of H_2TPP, AgTPP, and ZnTPP exhibit large distortions from the body-centered tetragonal cell (see Figure 10). While for most of the materials in Table Ib, a smaller guest is associated with a smaller *b*, these unsolvated species exhibit a large *b*. This expansion is accompanied, however, by a collapse of d_{002} from a typical value of ~4 Å to a value of ~2 Å.

Extended Porphyrin Chains. The materials in Figure 11 differ from all the species in previous sections in that the host repeat distance in the channel direction is expanded over the more typical 13–14-Å distance. This distortion of the host results in the loss of the presumably favorable interaction between orthogonal phenyl groups found in all other members of this series. This loss may be compensated for to some degree by an increased interaction among parallel phenyl groups on neighboring porphyrins. This extension of the *a* axis is in most cases accompanied by the introduction of a "zig-zag" pattern in the channel. It is difficult

---

(47) See note *f* in Table I.

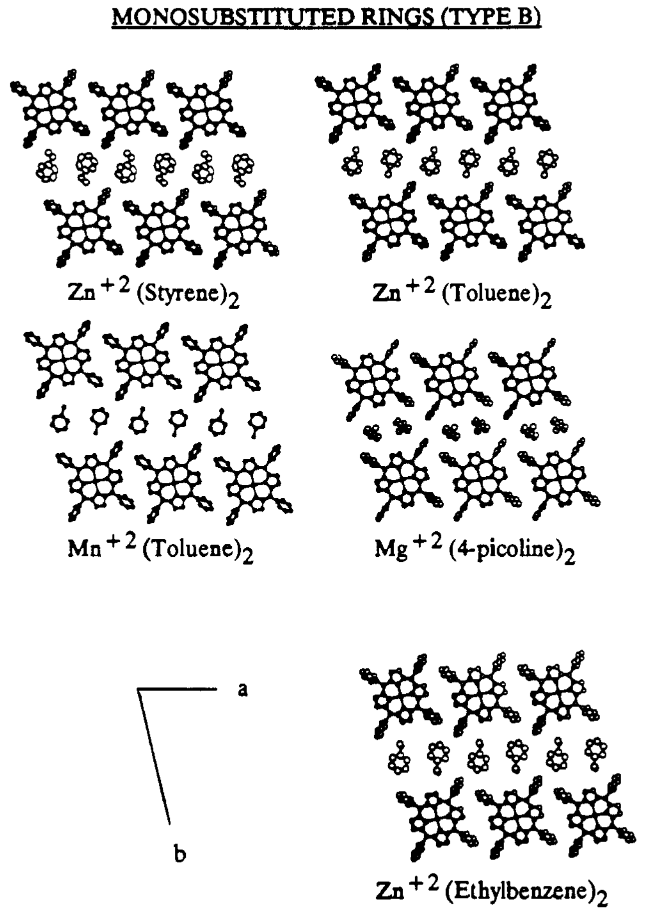
MONOSUBSTITUTED RINGS (TYPE B)

Zn^{+2} (Styrene)$_2$

Zn^{+2} (Toluene)$_2$

Mn^{+2} (Toluene)$_2$

Mg^{+2} (4-picoline)$_2$

Zn^{+2} (Ethylbenzene)$_2$

Figure 5. Porphyrin sponges containing monosubstituted six-membered rings (type B).

to ascribe this particular distortion to common features of the guests.

A Link between Triclinic and Tetragonal Structures. The structures in Figures 3–11 illustrate various modes of lattice distortion induced by the introduction of guest species. Some of these structures differ quite markedly from those of the tetragonal materials. On the other hand, the structure of triclinic Ru^{II}TPP(CO)(EtOH) exhibits a distinct similarity to those of the tetragonal materials (see Figure 12). The deviation of the ethanol ligand from axial symmetry appears to be sufficient to lower the lattice symmetry. As observed for the tetragonal materials, the axial ligands in this material reside at the intersection of the lattice channels in the *a* and *b* directions.

Occupation of Multiple Channels. The structure illustrated in Figure 13 differs from the others in that multiple channels are occupied. In this species, benzimidazole guests occupy the channel in the *a* direction, perchlorate counterions reside at the intersection of the *a* and *c* channels, and toluene guests reside at the intersection of the *b* and *c* channels.

Modeling. The large body of structural data available for the triclinic materials tabulated in Table Ib undoubtedly contains information that can be used empirically to model the way in which molecular size and shape govern guest orientation and host distortions in this system. At a higher level, such a model might be refined by application of the tools of molecular mechanics. Indeed, this system could prove useful in testing and improving these molecular mechanics methods.

Range of Composition. The compilation in Table I illustrates the broad composition range of materials in this class, from those with no ligands or solvates, to those with as many as 80 guest atoms per porphyrin molecule. At the present time there is no clear indication of the maximum size of the guest species. Saturated hydrocarbons and halocarbons are not usually incorporated, although chloroform and carbon tetrachloride are included in a few materials in which they participate in hydrogen-bonding networks with ionic ligands. All the guests in Figures 2–13 either contain a heteroatom that interacts with the metal atom or with a counterion or contain an unsaturated component that appears to interact in an attractive fashion with the π system of the porphyrin. It may be possible, however, to incorporate saturated hydrocarbon species in 5-coordinate hosts "programmed" to produce a solvate site of an appropriate size (vide infra).

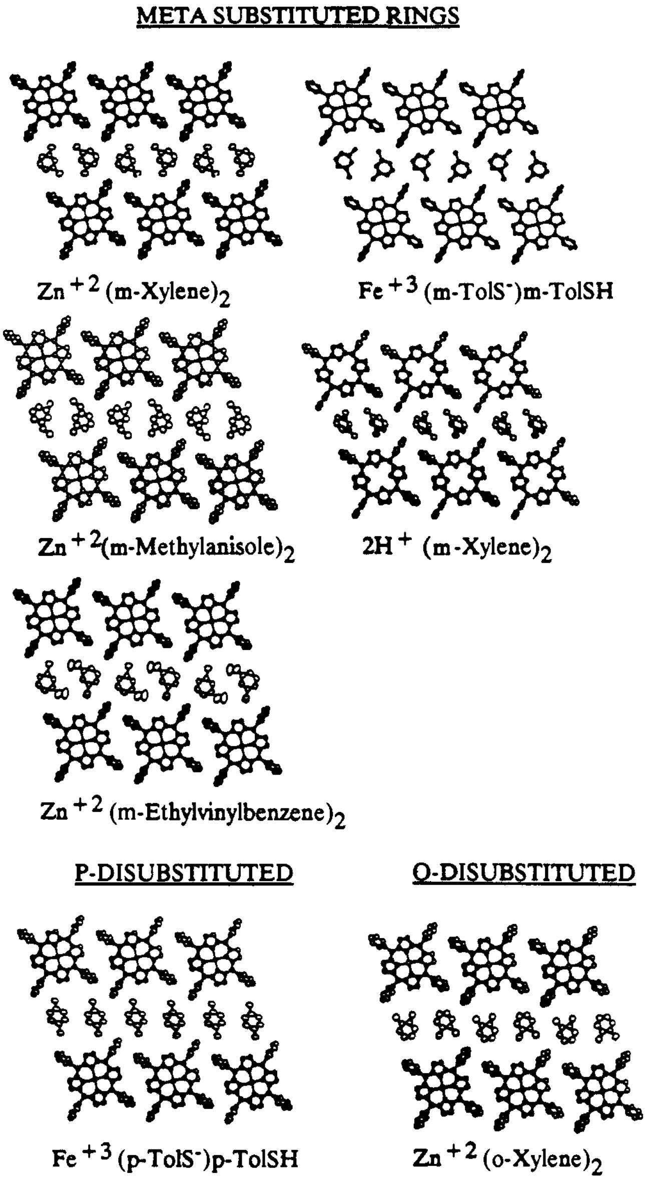
META SUBSTITUTED RINGS

Zn^{+2} (m-Xylene)$_2$

Fe^{+3} (m-TolS$^-$)m-TolSH

Zn^{+2}(m-Methylanisole)$_2$

2H$^+$ (m-Xylene)$_2$

Zn^{+2} (m-Ethylvinylbenzene)$_2$

P-DISUBSTITUTED

Fe^{+3} (p-TolS$^-$)p-TolSH

O-DISUBSTITUTED

Zn^{+2} (o-Xylene)$_2$

Figure 6. Porphyrin sponges containing disubstituted benzenes.

Eleven different metal atoms have been identified in these species in oxidation states ranging from 0 to +5. Metal atom coordination numbers of 4, 5, and 6 have been observed. In some materials the metal atoms have been replaced by two hydrogen atoms.

This lattice also accommodates substituted porphyrins; bromo substitution of the pyrrole groups and *o*-amino substitution of the porphyrin phenyl groups have yielded materials isostructural with the unsubstituted species.[48] Incorporation of spin-labeled porphyrins into a matrix of unsubstituted material has also been demonstrated (vide infra). Preliminary investigations of other substituted TPP complexes (vide infra) suggest that the TPP "sponges" tabulated in Table I may represent a very small sample of the full range of composition.

The fact that TPP complexes crystallize from a wide range of solvents with incorporation of guests must be a consequence of an unfavorable lattice energy associated with the unsolvated

---

(48) Reference 30 and unpublished results.

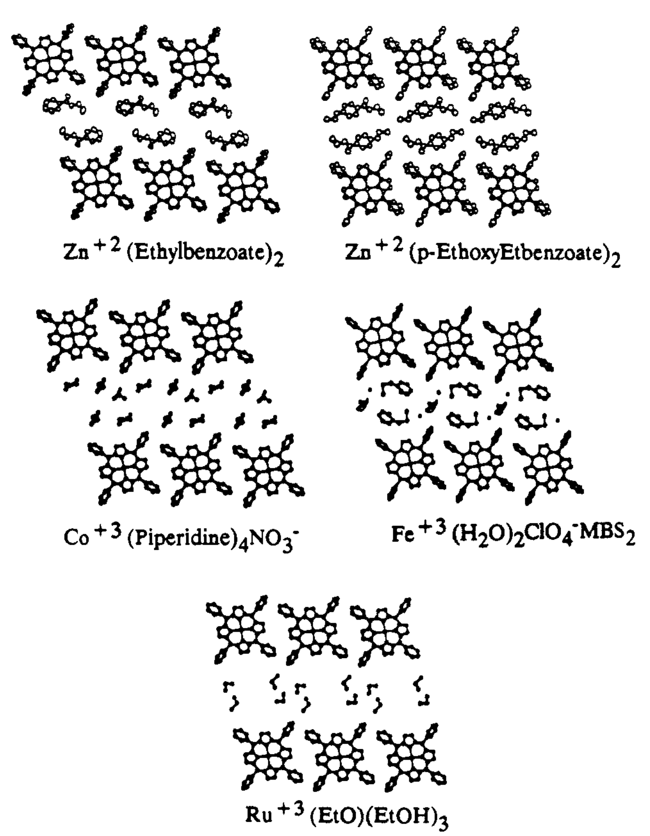

DOUBLE CHAINS

Zn^{+2} (Ethylbenzoate)$_2$ Zn^{+2} (p-EthoxyEtbenzoate)$_2$

Co^{+3} (Piperidine)$_4$NO$_3^-$ Fe^{+3} (H$_2$O)$_2$ClO$_4^-$MBS$_2$

Ru^{+3} (EtO)(EtOH)$_3$

Figure 7. Porphyrin sponges containing double chains of guests.

1:1 CLATHRATES

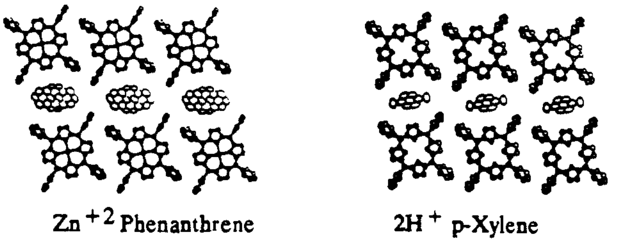

Zn^{+2} Phenanthrene 2H$^+$ p-Xylene

Figure 8. Porphyrin sponges with a 1:1 stoichiometry.

LARGE D_{002}

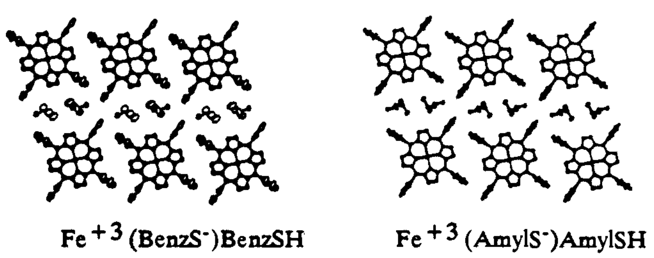

Fe^{+3} (BenzS$^-$)BenzSH Fe^{+3} (AmylS$^-$)AmylSH

Figure 9. Porphyrin sponges with a large interplanar spacing.

materials. This can be attributed at least in part to the rigidity of the TPP structure and the orthogonal orientation of the aryl groups with respect to the porphyrin plane.

While crystallization from some solvents gives a packing arrangement different from that illustrated in the preceding figures, solvent is usually incorporated; the majority of TPP structures in the 1988 Cambridge Structural Database[1] contain solvate molecules. For many clathrate applications, any solvate structure

DRY SPONGES

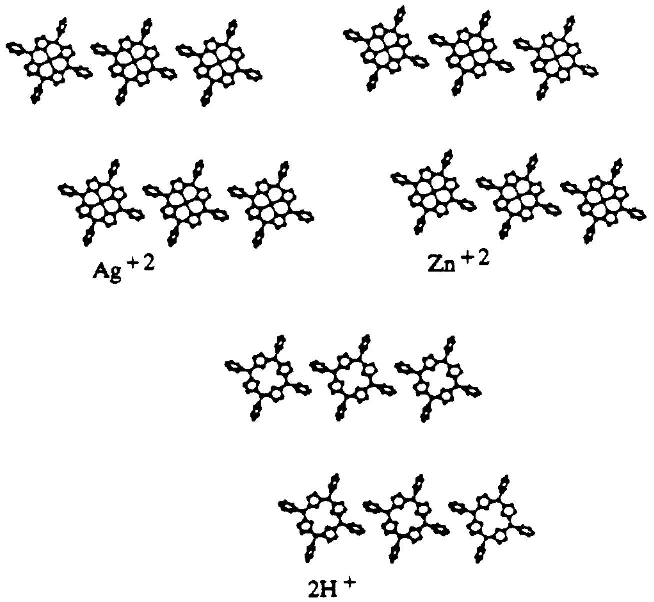

Ag^{+2} Zn^{+2}

2H$^+$

Figure 10. Unsolvated porphyrin sponges. The appearance of large empty channels in these drawings is somewhat misleading in that the channels are very shallow. In the absence of a guest, the host collapses along the c^* direction.

EXPANDED A

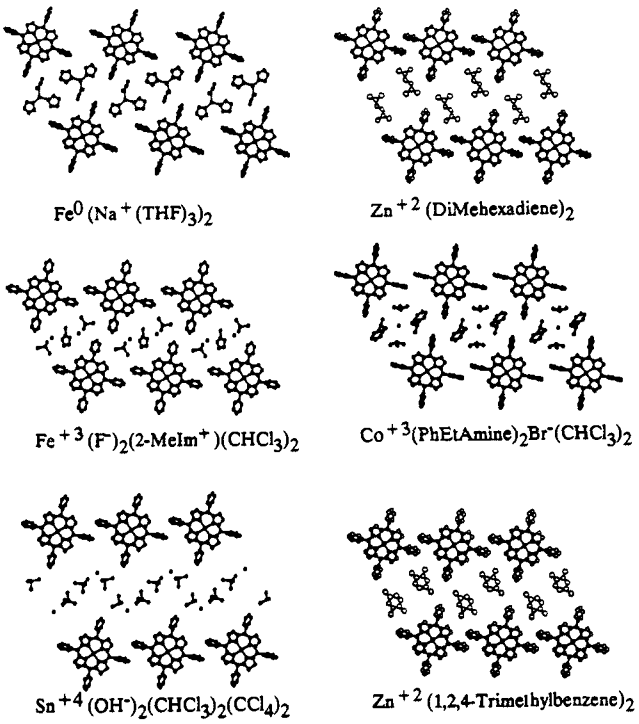

Fe^0 (Na$^+$(THF)$_3$)$_2$ Zn^{+2} (DiMehexadiene)$_2$

Fe^{+3}(F$^-$)$_2$(2-MeIm$^+$)(CHCl$_3$)$_2$ Co^{+3}(PhEtAmine)$_2$Br$^-$(CHCl$_3$)$_2$

Sn^{+4}(OH$^-$)$_2$(CHCl$_3$)$_2$(CCl$_4$)$_2$ Zn^{+2} (1,2,4-Trimethylbenzene)$_2$

Figure 11. Porphyrin sponges with extended porphyrin chains.

TETRAGONAL PSEUDOTETRAGONAL

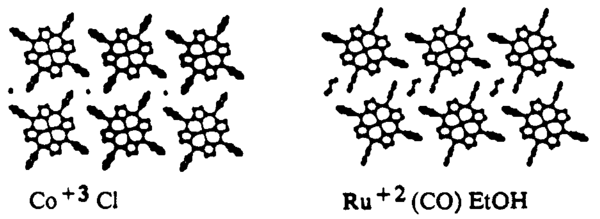

Co^{+3} Cl Ru^{+2}(CO) EtOH

Figure 12. Tetragonal and pseudotetragonal porphyrin sponges.

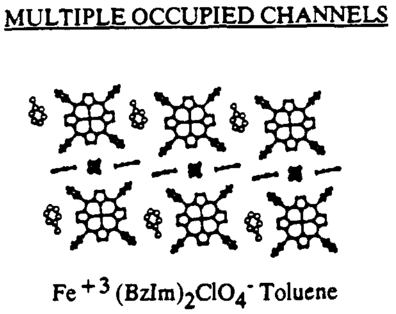

Figure 13. A porphyrin sponge with multiple occupied channels.

is usable. For applications where the triclinic 1:2 structure is desirable, it is sometimes possible to induce this form by seeding.

Applications. The "tetraarylporphyrin sponges" described herein offer a very versatile matrix that can be employed in a number of chemical and technological applications. In some of these applications, the fact that the matrix is constructed from porphyrin complexes is essential, while in others it is of no consequence. In this section, applications involving molecular recognition and chemical separations, matrix isolation, and adsorption/desorption are discussed. In the following section, potential applications involving polymer formation and photoactive devices are suggested.

Molecular Recognition and Chemical Separations. The diversity of TPP-based clathrates suggests an almost complete lack of specificity in the incorporation of guests into these hosts. Growth of high-quality crystals of ZnTPP containing most of the components of unleaded gasoline (vide infra) further supports this view.

There is, however, a simple route whereby such materials can be "programmed" to incorporate guests of a specific size, shape, handedness, and charge. This procedure is based on the observation that the materials in Table I include 4-, 5-, and 6-coordinate metalloporphyrins, all of which exhibit the same porphyrin framework (see Figure 14). In the structures of the 4-coordinate materials, solvate molecules occupy the open channels. With the 6-coordinate materials, the axial ligands occupy the channels. In both cases the metal atom resides on a crystallographic inversion center. In the 5-coordinate materials, the single axial ligand and one solvate molecule occupy alternate sites in the channel. Since to a large extent the packing is controlled by the centrosymmetric TPP molecule, the consequence of attaching a single axial ligand to the metal atom is the creation of a guest site with the same size and shape as the axial ligand but of opposite handedness. The axial ligand thus serves as an inverted template for the desired guest. Stated in another way, the centrosymmetric arrangement of the porphyrin ligands constrains the ligand site and the guest site to be related by a pseudoinversion center; solvate molecules of the same size and shape as the axial ligand (and for chiral species, those of opposite handedness) are likely to be preferentially incorporated.

This approach differs from molecular host/guest chemistry in that here one is tailoring a lattice, rather than a molecule, to act as a host. The chemistry involved is much simpler, because the same building blocks can be used to accommodate a wide range of guests. In the following, several preliminary examples of such axial ligand "programming" are described. A more detailed account of this effort will be published later.

Molecular Recognition: Example 1. As seen in Table II, when $Zn^{II}TPP$ is crystallized from a mixture of chlorobenzene and the three isomers of dichlorobenzene, the crystals produced contain various amounts of the three dichlorobenzenes and a smaller amount of chlorobenzene. On the other hand, when (2,5-dichlorophenolate)iron^{III}TPP is crystallized from the same mixture, 1,4-dichlorobenzene is incorporated with high specificity. This observation can be rationalized on the basis that the relative chlorine atom dispositions of the guest are the same as those of the ligand. When viewing the ligand as a template for the guest, one must discount to some extent the influence of the donor atom (in this case the phenolate oxygen atom) because a nonbonded atom related to the donor atom by the pseudoinversion would experience significant repulsion from the iron atom.

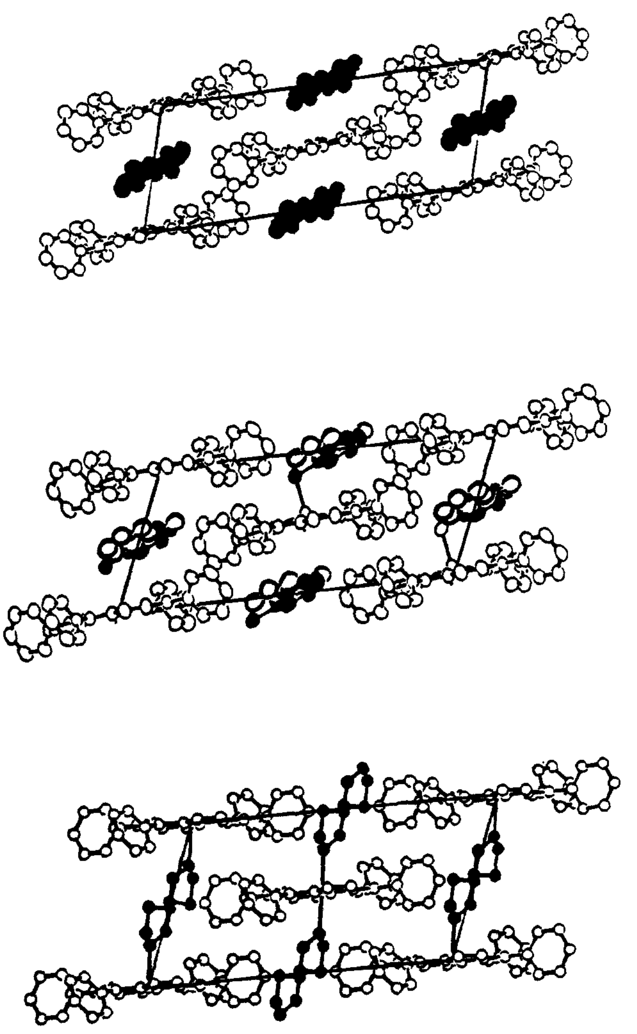

Figure 14. Packing diagrams viewed down the *a* axis for 4-, 5-, and 6-coordinate TPP complexes.

Table II. Crystallizations of TPP Hosts from Mixed Solvents. Gas Chromatographic Analysis of the Incorporated Solvent Expressed as Mole Fractions

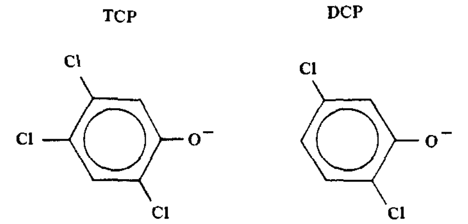

component	solv[a]	ZnTPP	FeTPP(DCP)[b]	FeTPP(TCP)[c]
		Experiment 1		
chlorobenzene	0.23	0.02	0.00	
o-dichlorobenzene	0.26	0.38	0.00	
m-dichlorobenzene	0.25	0.45	trace	
p-dichlorobenzene	0.26	0.14	1.00	
		Experiment 2		
p-xylene	0.49	0.08	0.79	0.28
1,2,4-trimethylbenzene	0.51	0.92	0.21	0.72
		Experiment 3		
p-xylene	0.31	0.81	0.09	
p-chlorotoluene	0.34	0.13	0.31	
p-dichlorobenzene	0.35	0.06	0.60	

[a] Gas chromatographic analysis of the starting solvent. [b] DCP, 2,5-dichlorophenolate. [c] TCP, 2,4,5-trichlorophenolate.

Molecular Recognition: Example 2. The second section of Table II describes the incorporation of a mixture of *p*-xylene and

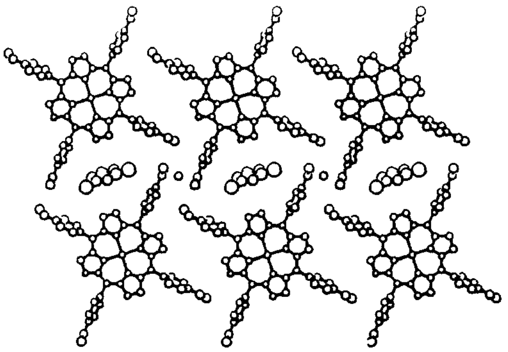

Figure 15. Crystal structure of tetraanisylporphinatozinc(II)·H_2O·*m*-xylene.

1,2,4-trimethylbenzene in three different TPP hosts. As in the previous example, the ZnTPP preferentially incorporates the larger solvate. On the other hand, (2,5-dichlorophenolate)iron^{III}TPP preferentially incorporates *p*-xylene and (2,4,5-trichlorophenolate)iron^{III}TPP preferentially incorporates trimethylbenzene. These results can again be rationalized on the basis of the similarity in the size and shape of the ligand and solvate.

Molecular Recognition: **Example 3.** The last section of Table II describes the incorporation of a mixture of *p*-xylene, *p*-chlorotoluene, and *p*-dichlorobenzene into ZnTPP and (2,5-dichlorophenolate)iron^{III}TPP hosts. It is observed that the Zn host shows a preference for the alkylated guests while the iron host shows a preference for the chlorinated guests. This difference is probably best rationalized on the basis of a difference in host polarity, the more polar hosts selecting the more polar guests and vice versa. This represents another way in which the host can be programmed to accommodate a particular class of guests.

Other Types of Programming. In addition to the attachment of an axial ligand, there are other ways in which these materials can be programmed to carry out specific chemical separations. One involves alteration of the oxidation state of the metal atom, which in the materials tabulated above ranges from 0 to +5. The use of a +2 metal oxidation state results in the incorporation of neutral solvates and/or ligands, while lower charges require the incorporation of cations and higher charges require the incorporation of anions.

For applications of these materials in chemical separations, the porphyrin phenyl groups can be substituted to change the solubility properties of the host and to develop specific interactions between hosts and guests. While all the porphyrins illustrated in Figures 2–13 are unsubstituted, Figure 15 shows the packing of a ZnTPP complex with methoxy substituents on the phenyls. Although this material is monoclinic, it exhibits much the same two-dimensional packing arrangement as the unsubstituted porphyrins.[46]

Matrix Isolation. This general class of applications includes the use of these "sponges" to immobilize and isolate molecular species. These species can either be guest molecules that reside in the channels formed by the porphyrin host or they can be porphyrin molecules that differ chemically from the bulk of the host. Incorporation of the guest molecule has the effect of immobilizing it in an ordered array, as well as greatly reducing its interactions with neighboring guests.

From a more macroscopic point of view, one application of these materials involves the transformation of liquids to crystalline solids. Such a transformation might be desired to facilitate structural characterization of the guest, or to simplify its handling and storage. Whatever the reason, the desired transformation can usually be affected simply by recrystallizing an appropriate TPP complex from the liquid of interest.

Matrix Isolation: **Example 1.** In a simple but illustrative example of transformation of a liquid to a solid, ZnTPP was crystallized from a sample of unleaded gasoline. High-quality crystals were obtained. Thermogravimetric analysis revealed that these crystals contained approximately 23% by weight solvent. Gas chromatography of the low-boiling material extracted from these crystals revealed that most of the components of gasoline were present in the crystals (see Figure 16). Parallel experiments with binary mixtures of xylenes suggest that these crystals are homogeneous; i.e., single crystals of ZnTPP grown from a mixture of xylenes were found to have a solvate composition similar to that of the mother liquor.

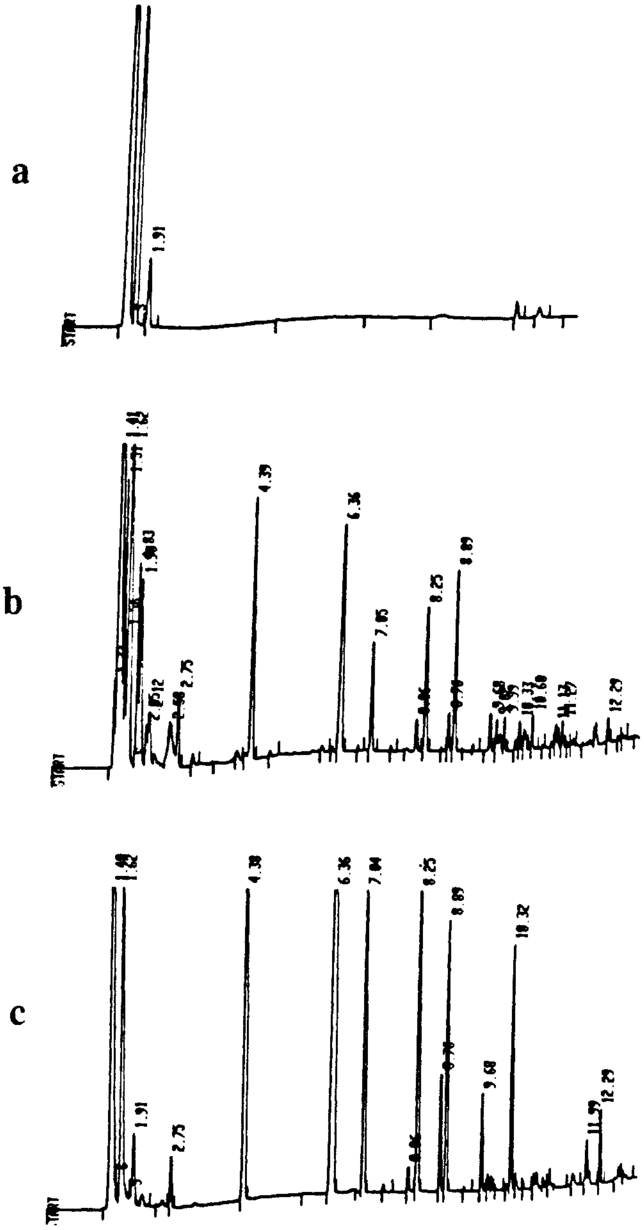

Figure 16. Gas chromatographic analyses of ZnTPP crystals grown from unleaded gasoline. (a) Solvent blank. (b) Unleaded gasoline. (c) Extract from ZnTPP crystals.

Matrix Isolation: **Example 2.** For materials that are liquids at room temperature, single-crystal investigations are often difficult. Handling difficulties can be greatly reduced by incorporation of the small molecule into a "sponge". In one such investigation, the X-ray structure determination of the 1,5-cyclooctadiene solvate of ZnTPP tabulated in Table I was undertaken to obtain accurate structural parameters for the guest.[49]

This approach might be especially useful in the study of dynamic conformational interconversion in small molecules (e.g., cyclic hydrocarbons). Such studies are often complicated by cooperative interactions in the pure materials. These interactions often result in a large number of phase transitions, many of which are difficult to characterize. By locking the molecule of interest in a "sponge",

---

(49) The use of the free porphyrin rather than the metalloporphyrin would probably provide even more accurate structural data.

these cooperative interactions can be greatly reduced. Any "site" influence on the thermodynamics can be examined by systematic variation of the host. While no investigation has been initiated solely to exploit this type of dilution, it has been observed[50] that the chlorobenzene solvate in Fe^{III}TPP(benzenethiolate)·chlorobenzene is dynamically disordered between at least two orientations at room temperature. At 125 K only a single orientation is observed.

Matrix Isolation: Example 3. An application involving a somewhat different kind of dilution is provided by the study of a mixed chlorobenzene/benzenethiol solvate of Fe^{III}TPP(benzenethiolate).[50] In investigations of dynamic interconversions (e.g., the spin-state equilibrium of FeTPP(benzenethiolate)(benzenethiol), analysis of the thermodynamics is greatly simplified if cooperative interactions can be eliminated. This can be accomplished if the active species is diluted in some inactive host. For this spin equilibrium, dilution of the benzenethiol solvate with the chlorobenzene solvate produces no significant change in the temperature of the transition, suggesting that the transition in the pure material is not cooperative. This lack of cooperativity is probably another manifestation of the fact that the packing in these materials is governed primarily by porphyrin–porphyrin interactions.

Matrix Isolation: Example 4. A final application involving dilution is the preparation of magnetically dilute single crystals. The hyperfine splitting tensors, available from EPR measurements of magnetically dilute single crystals, can provide a detailed picture of the electronic structure of either a porphyrin complex or a paramagnetic guest. The use of Zn^{II}TPP, either as the 4-coordinate toluene solvate or as a 6-coordinate complex with neutral ligands, is particularly attractive for this purpose. The fact that these materials are triclinic with $Z = 1$ makes them especially useful for single-crystal spectroscopy. The feasibility of such dilutions has been demonstrated very effectively by a series of investigations by Eaton, Eaton, and co-workers.[51] They prepared dilute crystals of spin-labeled porphyrin complexes in ZnTPP-$(THF)_2$. In these complexes, the spin label attached to the porphyrin presumably occupies one of the channels, probably displacing one or more THF molecules. It was found that in most cases the label could adopt a number of conformations in the lattice.

Matrix Isolation: Example 5. In another application to porphyrin chemistry, these materials offer a crystalline matrix for the isolation and study of metalloporphyrin complexes of very weak ligands. Cooling a "sponge" in which potential ligands have been incorporated as solvate molecules will, in some cases, result in the formation of complexes that are amenable to crystallographic and spectroscopic study. A preliminary account of the application of this technique to the study of the coordination of benzenethiol to Fe^{III}TPP(benzenethiolate), with concomitant spin transformation, has been published.[52]

Desorption and Adsorption. Another class of applications involves the active exchange of ligands and/or solvate molecules in a preformed "sponge". It is certainly possible to perform a bulk extraction of the solvate molecules and neutral ligands. In most cases such an extraction will result in loss of crystallinity, but the high surface area material so formed can be very reactive. Sorrell and Collman used such a procedure to prepare mixed-ligand amine/thiolate complexes.[53] Vacuum treatment of ferric benzenethiolate complexes at elevated temperature results in extraction of the ligand in the form of diphenyl disulfide with transfer of an electron to form Fe^{II}TPP, again presumably in a high surface area form.

Exchange of solvate molecules and/or ligands without loss of crystallinity would open up another range of applications.

Potential Applications. Polymers. The channel structure observed in Figures 3–13 suggests the possibility of using these materials to produce stereoregular polymers. Similar polymerizations have been carried out in the channels of urea- and thiourea-based clathrates.[54] The existence of the material in Figure 13 suggests the possibility of constructing a two- or three-dimensional network of monomers in the porphyrin channels.

While the TPP-based host appears attractive because of the wide range of monomers that can be incorporated, this same flexibility of the host greatly reduces orientational freedom of the guests. That is, a polymerization that requires considerable reorientation of the monomer is unlikely to take place in the TPP host.

Another type of polymerization that would be of considerable interest, and which might be used to deal with the problem of limited guest motion, is a polymerization that involves the host molecules. If the host molecules could be linked into a rigid network in the presence of some inert guest, removal of the guest would leave a preformed network of channels into which new guests could be introduced. This might be used to produce a new class of size-selective membranes.

Photosystems. The light-harvesting properties of porphyrin derivatives are used extensively by nature. It should be possible to take advantage of the unique properties of porphyrin sponges to construct some useful photoactive devices. If, for example, it proved possible to construct a conjugated polymer within one of the sponge channels, it might be possible to produce a programmable photoconductor. By doping the host porphyrin with a small amount of porphyrin having a lower lying excited state, one would produce the analogue of a photosynthetic reaction center that could efficiently trap photoexcitation. This excited trap could then transfer an electron to the polymer, hence altering its electrical properties. The lifetime of the charge-separated state in such a device could be controlled by changing the nature and concentration of the trap species.

Conclusions

Porphyrin–porphyrin interactions dominate the crystal packing of tetraphenylporphyrin complexes, as witnessed by the fact that the same gross packing arrangement is preserved in over 65 TPP complexes. In this packing arrangement, parallel chains of porphyrin molecules surround extended channels. The fact that the axial coordination sites of the metalloporphyrin metal atoms are directed into these channels allows one to exercise considerable control over the channel contents. Addition of a single axial ligand can be used to "program" one of these hosts for the preferential incorporation of guest species of a predetermined size, shape, handedness, and charge. Preliminary investigations have demonstrated the feasibility of a range of scientific and technological applications of these unusual lattice clathrates.

Acknowledgment. This work was supported by the National Science Foundation (CHE 87-06780) and the National Institutes of Health (GM 35329), and by a UCLA BRSG grant. We thank students in the Chemistry 277 and 184 classes at UCLA and in the UCLA Engineering Minority Recruitment Program who participated in some of the research reported herein.

Supplementary Material Available: Transformations from the unit cells in which the structures are reported to the unit cell tabulated in Table I and crystallographic and refinement data, structures, positional parameters, isotropic and anisotropic temperature factors, interatomic distances, and bond angles for ZnTPP clathrates of the guests benzene, styrene, phenylacetylene,

---

(50) The next paper in this series[32] reports a detailed multiple-temperature structural analysis of several 5-coordinate "sponge" materials. That paper demonstrates the nonstandard crystallographic techniques whereby the structures of these intrinsically disordered materials can be accurately determined.

(51) Damoder, R.; More, K. M.; Eaton, G. R.; Eaton, S. S. *J. Am. Chem. Soc.* **1983**, *105*, 2147–2154.

(52) Collman, J. P.; Sorrell, T. N.; Hodgson, K. O.; Kulshrestha, A. K.; Strouse, C. E. *J. Am. Chem. Soc.* **1977**, *99*, 5180–5181.

(53) Collman, J. P.; Sorrell, T. N.; Hoffman, B. M. *J. Am. Chem. Soc.* **1975**, *97*, 913–914.

(54) (a) Clasen, H. *Z. Elektrochem.* **1956**, *60*, 982. (b) Brown, J. F.; White, D. M. *J .Am. Chem. Soc.* **1960**, *82*, 5671. (c) White, D. M. *J. Am. Chem. Soc.* **1960**, *82*, 5678.

ethylbenzene, 1,2,4-trimethylbenzene, 1-ethyl-3-vinylbenzene, phenanthrene, 3-methylanisole, methyl benzoate, ethyl benzoate, ethyl 4-ethoxybenzoate, trioxane, 2,5-dimethyl-2,4-hexadiene, 1,5-cyclooctadiene, and the three isomers of xylene, for H_2TPP clathrates of *p*-xylene and *m*-xylene, and for the tetraanisylporphinatozinc(II) clathrate containing *m*-xylene and water (287 pages). Ordering information is given on any current masthead page.

Reaction of Carbon Monoxide with Alkyliron Porphyrins Generated from Alkyl Halides and Electrochemically Produced Iron(I) and Iron("0") Porphyrins

Claire Gueutin,[1a] **Doris Lexa,**[1a] **Michel Momenteau,**[1b] **and Jean-Michel Savéant***,[1a]

Contribution from the Laboratoire d'Electrochimie Moléculaire de l'Université Paris 7, Unité de Recherche Associée au CNRS No. 438, 2, Place Jussieu, 75251 Paris Cedex 05, France, and Institut Curie, Section de Biologie, Unité INSERM 219, 91405 Orsay, France.

Received June 5, 1989

Abstract: Carbon monoxide inserts in iron–carbon bonds of σ-alkyl porphyrins generated from the reaction of alkyl halides with electrochemically produced low-valent iron porphyrins, with the exception of benzyl derivatives. In the case of σ-aryl complexes, the iron–carbon appears too strong to allow CO insertion. In the case of methyl and other primary alkyls, CO insertion occurs at the Fe(III)–C rather than at the Fe(II)–C oxidation state. Insertion is then accompanied by partial homolysis of the σ-alkyl–Fe(III) complex favored by the binding of CO to the resulting iron(II) porphyrin. The latter reaction prevents the insertion of CO in the iron(III)-*tert*-butyl complex. However, CO then inserts in the Fe(II)–C-*tert*-butyl bond. The reaction mechanism is established and the characteristic rate constants are estimated on the basis of cyclic voltammetry, thin-layer spectroelectrochemistry, and preparative-scale electrolysis.

The reaction of alkyl halides with iron(I)[2a] and iron("0")[2b] porphyrins is a facile route to the corresponding σ-alkyl porphyrin complexes, even with sterically encumbered[2d] carbon and/or iron centers.[2] On the other hand, electrochemical reduction is a convenient way to in situ generate these low-valent complexes from the corresponding iron(III) porphyrins.[2] In a preliminary report,[3a] we have provided evidence that carbon monoxide inserts in the carbon–iron bond of such σ-alkyl porphyrins as in the case of ethyl and *n*-hexyl and of octaethylporphyrin (OEP). It was also shown that insertion occurs with the σ-alkyl complex in its iron(III) oxidation state rather than in its iron(II) oxidation state.[3a] Direct insertion of carbon monoxide in the carbon–iron bond of σ-ethyl-, *n*-butyl-, and neopentyliron(III)–tetraphenylporphyrin complexes obtained from the corresponding alkyllithiums and chloroiron(III) porphyrins has also been demonstrated in an independent preliminary report.[3b]

The purpose of the present paper is to provide a fuller account of the reaction of carbon monoxide with electrochemically generated σ-alkyliron porphyrins as a function of the nature of the alkyl group, so as to precisely determine the conditions under which this "nonmigratory" insertion[3c] can take place and investigate the reaction mechanism. The case of σ-aryliron porphyrins will be also briefly examined.

Results and Discussion

Most of the experiments were carried out with OEP, although a few test experiments were carried out with other porphyrins.

It has been shown, in a previous preliminary report,[3a] that electrolysis of $(OEP)Fe^{III}$ at a potential where the $Fe(I)^-$ complex is generated, in the presence of *n*-hexyl bromide and carbon monoxide, results in the formation of the corresponding iron(II)-acyl complex. The latter was identified by means of its spectral (UV-vis, IR, ^{13}C NMR) and electrochemical (cyclic voltammetry) behavior. Since then, we have found that the same reaction occurs with other primary alkyl halides (the particular case of methyl chloride is discussed below). The acyl complexes thus obtained have the same characteristics as those formed by the reaction of $Fe(\text{"0"})^{2-}$ porphyrins with carboxylic anhydrides.[5] In this preliminary study,[3a] CO insertion in the primary carbon–iron bond was investigated by cyclic voltammetry and thin-layer spectroelectrochemistry of solutions containing a mixture of the iron(III) porphyrin, the alkyl halide, and carbon monoxide. On the other hand, Goff et al.[3b] investigated the reaction starting from σ-alkyliron(III) porphyrins. In order to investigate the reaction mechanism and kinetics in more detail, we started in the present study from pure solutions of the σ-alkyliron(II) complex. Thanks to the volatility of ethyl bromide, this is most convenient

---

(1) (a) Université Paris 7. (b) Institut Curie.

(2) (a) Lexa, D.; Mispelter, J.; Savéant, J.-M.; *J. Am. Chem. Soc.* **1981**, *103*, 6806. (b) Lexa, D.; Savéant, J.-M.; Wang, D. L. *Organometallics* **1986**, *5*, 1428. (c) The reaction of alkyl halides with iron(I) porphyrins[2a] yields the $Fe^{III}R$ complex in a first stage. However, this is easier to reduce than the iron(II) porphyrin. Thus, at the potential where the $Fe^{III}R$ complex is produced, it is reduced to the $Fe^{II}R^-$ complex unless other reactions compete favorably. The reductant is in most practical cases the iron(I) complex rather than the electrode since alkylation is not sufficiently fast for the second event to occur. On the other hand, reaction of iron("0") porphyrin with alkyl halides directly yields the $Fe^{II}R^-$ complex. (d) Gueutin, C.; Lexa, D.; Savéant, J.-M.; Wang, D. L. *Organometallics* **1989**, *8*, 1607. (e) For a discussion of the reaction mechanism, dissociative electron transfer followed by bond formation or S_N2 substitution. See ref 2f. (f) Lexa, D.; Savéant, J.-M.; Su, K. B.; Wang, D. L. *J. Am. Chem. Soc.* **1988**, *110*, 7617.

(3) (a) Gueutin, C.; Lexa, D.; Savéant, J.-M.; Momenteau, M. *J. Electroanal. Chem. Interfacial Electrochem.* **1988**, *256*, 219. (b) Arafa, I. M.; Shin, K.; Goff, H. M. *J. Am. Chem. Soc.* **1988**, *110*, 5228. (c) "Nonmigratory"[3b] as opposed to the more common case where the inserting group is coordinated to the metal in cis vis-à-vis the alkyl group thus allowing an easy intramolecular migration of the latter toward the former.[4]

(4) (a) Alexander, J. J. In *Chemistry of the metal-carbon bond*; Hartley, F. R., Patai, S., Eds.; Interscience: New York, 1985; Vol. 2, p 339. (b) Stoppioni, P.; Dapporte, P.; Sacconi, L. *Inorg. Chem.* **1978**, *17*, 718. (c) Garrou, P. E.; Heck, R. F. *J. Am. Chem. Soc.* **1976**, *98*, 4115.

(5) Gueutin, C.; Lexa, D.; Savéant, J.-M. *J. Electroanal. Chem. Interfacial Electrochem.* **1988**, *256*, 223.

0002-7863/90/1512-1874$02.50/0